# Double-Regge-Pole Analysis of $\pi^+p \to \pi^+\rho^0 p$ at 13.1 GeV/$c$*

J. A. GAIDOS, C. R. EZELL, J. W. LAMSA, AND R. B. WILLMANN
*Purdue University, Lafayette, Indiana 47907*
(Received 21 May 1970)

A double-Regge-exchange analysis of the reaction $\pi^+p \to \pi^+\rho^0 p$ at 13.1 GeV/$c$ is presented. The events are divided into proton diffractive (~80%) and pion diffractive (~20%) categories, each of which requires two double-Regge amplitudes for a complete description. The data of each sample are well described by a double-Regge model consistent with duality.

## INTRODUCTION

PERIPHERAL production of three-particle final states has recently received much experimental and theoretical attention. The possibility of analyzing these reactions in terms of a multiperipheral model stemming from studies of peripheral two-body final states has been partially realized in terms of Regge exchanges. Arguments based on the duality concept have provided qualitative justification for the application of peripheral amplitudes in kinematical regions where their validity has been dubious. A representative, but not complete, list of some of the reactions previously studied in terms of a double-peripheral model include $K^+p \to K^+\omega p$ and $K^+\phi p$ at 9.0 and 4.6 GeV/$c$ by Alexander *et al.*,[1] $K^+p \to K^{*0}\pi^+p$ at 12.7 GeV/$c$ by Yuta[2] and at 7.3 GeV/$c$ by Chien *et al.*,[3] $K^-p \to K^{*0}\pi^-p$ and $K^-\Delta^{++}\pi^-$ at 12.6 GeV/$c$ by Anderws *et al.*,[4] $K^-p \to K^{*0}\pi^-p$ at 7.3 GeV/$c$ by Chung *et al.*,[5] $\pi^-p \to \pi^-\rho^0 p$ at 13.0 and 20.0 GeV/$c$ by Ioffredo *et al.*,[6] $\pi^-p \to \pi^-\pi^-\Delta^{++}$ at 6 GeV/$c$ by Mott *et al.*,[7] and $pp \to \Delta^{++}\pi^-p$ and $pp\omega$ at 19 GeV/$c$ by Høyrup,[8] and at 16 GeV/$c$ by Rushbrooke and Williams.[9]

In this paper we present data on the $\pi^+\rho^0 p$ final state at 13.1 GeV/$c$ and use a double-Regge amplitude to provide a simple model to describe the data. The choice of amplitudes and forms is based upon simplicity and the parametrization is not necessarily unique. Of particular interest is the interpretation of the low-mass $\pi$-$\rho$ enhancement, referred to as the $A$ region, as a result of peripheral dynamics or as a resonant state, or perhaps both. The $A$ region, $M(\rho\pi) \sim 0.9 \to 1.4$ GeV, is characterized by a broad diffractively produced peak of 90% $1^+$ $s$-wave $J^P$ component.[10]

## EXPERIMENTAL RESULTS

The data were obtained through a 230 000 picture exposure of the SLAC 82-in. hydrogen bubble chamber to a 13.1-GeV/$c$ separated $\pi^+$ beam, with a path length equivalent to ~9 events/$\mu$b. Of some 60 000 four-prong events measured on SMP's (scanning and measuring projectors) and processed by the local version of the TVGP-SQUAW analysis programs, approximately 10 000 were fitted according to the four-constraint $\pi^+\pi^+\pi^-p$ final-state hypothesis, with a $\chi^2$ probability of greater than 0.1%. The most conspicuous features of the four-particle final state were strong $\rho^0$, $f^0$, and $\Delta^{++}$ two-body formations and the clustering of the three-pion mass spectrum toward low values. The three-pion mass distribution is shown in Fig. 1 with the hatched portion representing the data with the $\Delta^{++}$ removed; the $\Delta^{++}$ was defined as those events with $1.136 < M(\pi^+p) < 1.336$ GeV.

For the subsequent analysis in this paper, a $\pi^+\pi^-$ combination was accepted as a $\rho$ if its invariant mass fell within a 0.2-GeV band centered at 0.765 GeV; background under the $\rho$ was estimated at less than

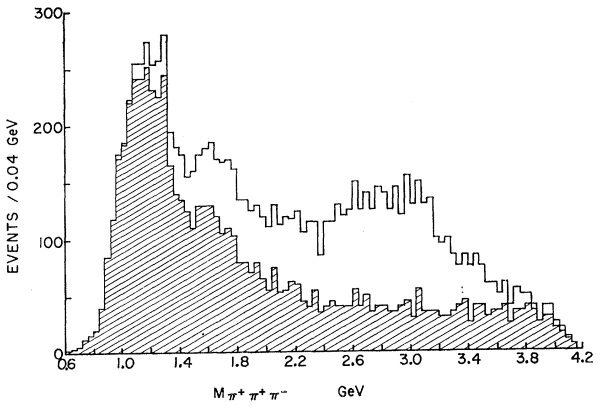


FIG. 1. Effective-mass distribution of the $\pi^+\pi^+\pi^-$ final states; hatched portion remains after $\Delta^{++}$ events are removed.

* Work supported by the U. S. Atomic Energy Commission.

[1] G. Alexander, A. Firestone, C. Fu, G. Goldhaber, and A. Pignotti, Phys. Rev. **177**, 2092 (1969).

[2] H. Yuta, University of Rochester Report No. 875-271 (unpublished); M. S. Farber, T. Ferbel, P. F. Slattery, and H. Yuta, Phys. Rev. Letters **22**, 1394 (1969).

[3] C. Y. Chien, E. I. Malamud, D. J. Mellama, F. D. Rudnick, P. E. Schlein, W. E. Slater, D. H. Stork, H. K. Ticho, and T. G. Trippe, Phys. Letters **29B**, 433 (1969).

[4] J. Andrews, J. Lach, T. Ludlam, J. Sandweiss, H. D. Taft, and E. L. Berger, Phys. Rev. Letters **22**, 731 (1969).

[5] S. U. Chung, R. L. Eisner, N. F. Bali and D. Lüers, Phys. Rev. **182**, 1443 (1969).

[6] M. L. Ioffredo, G. W. Brandenburg, A. E. Brenner, B. Eisenstein, L. Eisenstein, W. H. Johnson, Jr., J. K. Kim, M. E. Law, B. M. Salzberg, J. H. Scharenguivel, L. K. Sisterson, and J. J. Szymanski, Phys. Rev. Letters **31**, 1212 (1968).

[7] J. E. Mott, H. J. Martin, and K. F. Galloway, Nucl. Phys. **B16**, 102 (1970).

[8] Jens Høyrup, Nucl. Phys. **B11**, 428 (1969).

[9] J. G. Rushbrooke and J. R. Williams, Phys. Rev. Letters **22**, 248 (1969).

[10] A spin-parity analysis for the $A$ region will be published soon.

TABLE I. Kinematical definitions.

$$P_\pi + P_p \to k_\pi + k_\rho + k_p$$
$$s_{ab} = (k_a + k_b)^2 \quad a, b = \pi, \rho, p$$
$$t_{\pi a} = (P_\pi - k_a)^2$$
$$t_{pa} = (P_p - k_a)^2$$

25%. For less than 20% of the events in the $A$ region, both $\pi^+\pi^-$ combinations fell within the $\rho$ band. In this case, the mass combination closer to the central value was chosen. The choice of the alternate pair as the $\rho$ produced no noticeable change in the results. The $\pi^+ p$ invariant mass was restricted to values greater than 2.0 GeV in order to avoid complications with the $\Delta^{++}$ state. This selection of data yielded 3100 events.

The data sample is characterized by low four-momentum transfers from the beam to each of the outgoing bosons and from the target to the outgoing proton. The kinematical relation $S_{\pi\rho} + t_{\pi\pi} + t_{\pi\rho} = m_\rho^2 + 2m_\pi^2 + t_{pp}$ (see Table I for definitions) suggests that if a dynamical model can be formulated, i.e., if allowed exchange graphs can be found such that $t_{\pi\pi}$, $t_{\pi\rho}$, and $t_{pp}$ are simultaneously peaked toward small values, the mass squared of the $\pi$-$\rho$ system will necessarily have a low-mass enhancement. Conversely, if there is a low-mass resonance in the $\pi$-$\rho$ system, the four-momentum transfers $t_{\pi\pi}$ and $t_{\pi\rho}$ will be small, since the three-pion final state can be produced diffractively off the nucleon. We will show that simple exchange graphs which reproduce the data can occur in a natural way.

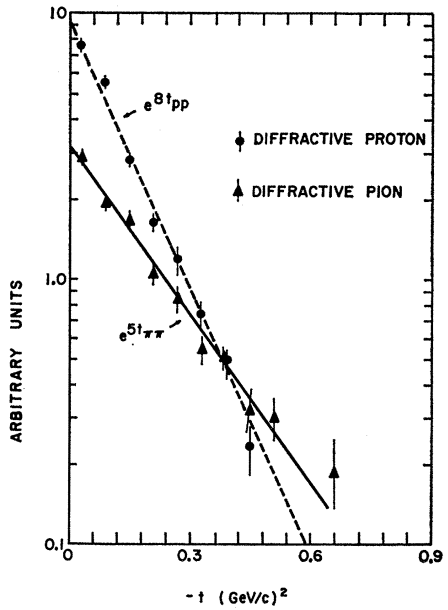


FIG. 3. Differential distribution of four-momentum transfers at the proton and pion diffractive vertices.

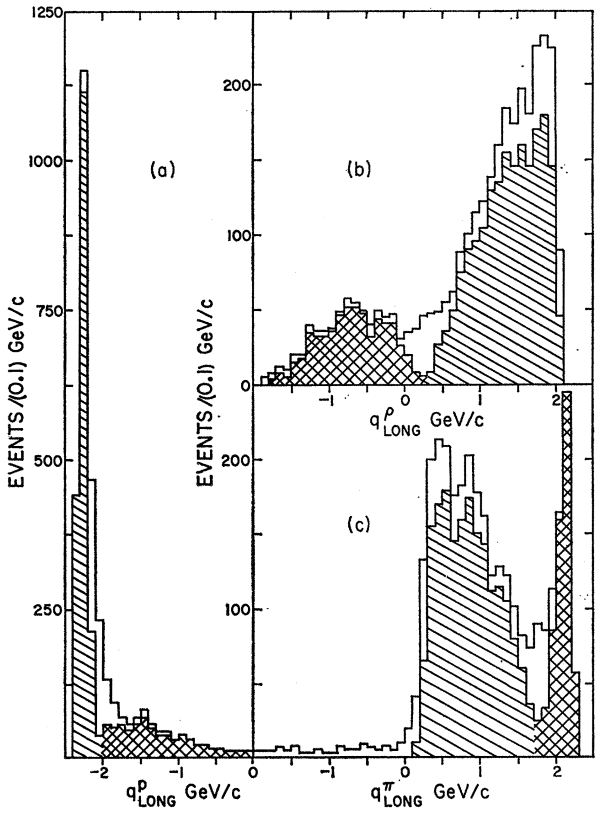


FIG. 2. Center-of-mass longitudinal momentum distributions. Diagonal hatching indicates the proton diffractive sample, cross hatching the pion diffractive sample.

The center-of-mass longitudinal momentum distributions of the proton, $\rho$ meson, and pion are shown in Fig. 2. Evidence for diffractive scattering of the target proton can be seen in Fig. 2(a), where the final proton distribution exhibits a sharp backward peak for $q_{\text{long}}{}^p < -2.0$ GeV/$c$, characteristic of a highly peripheral interaction. The sharp forward peak in the longitudinal momentum of the pion, $q_{\text{long}}{}^\pi$, shown in Fig. 2(c), similarly indicates diffractive scattering of the incident pion. The double-bumped structure in the longitudinal momentum of the $\rho$ in Fig. 2(b) arises from the separation of the events into proton diffractive and pion diffractive categories, the more forward bump being associated with proton diffraction. The data

TABLE II. Limits of regions to which double-Regge-pole analysis was applied. Proton diffractive events defined by $q_{\text{long}}{}^p < -2$ GeV/$c$, pion diffractive by $q_{\text{long}} > -2$ GeV/$c$.

| $q_{\text{long}}{}^p < -2$ GeV/$c$ | $q_{\text{long}}{}^p > -2$ GeV/$c$ |
|---|---|
| $-t_{\pi\pi} < 1.0$ (GeV/$c$)$^2$ | $-t_{\pi\pi} < 1.0$ (GeV/$c$)$^2$ |
| $-t_{\pi\rho} < 2.0$ (GeV/$c$)$^2$ | $-t_{pp} < 3.6$ (GeV/$c$)$^2$ |
| $-t_{pp} < 0.5$ (GeV/$c$)$^2$ | $-t_{pp} < 2.0$ (GeV/$c$)$^2$ |
| $M_\pi + p > 2.0$ GeV | $M_\pi + p > 2.0$ GeV |
| 1828 events | 550 events |

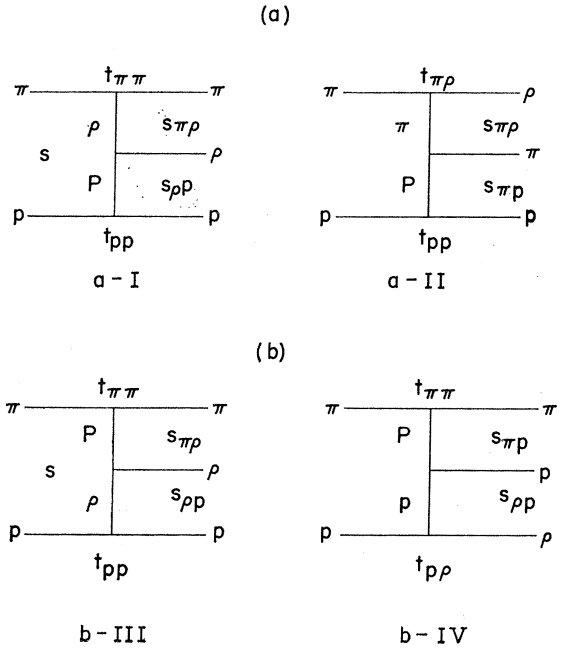


FIG. 4. Double-Regge diagrams used to describe (a) the proton diffractive data and (b) the pion diffractive data.

displayed in Fig. 2 suggest that most of the events in the $\pi^+\rho^0 p$ final state are produced by diffractive scattering off the pion or nucleon. In order to separate the contributions of the two diffractive vertices, a division of the data was made at $q_{\text{long}}{}^p = -2.0$ GeV/$c$; those events with $q_{\text{long}}{}^p < -2.0$ GeV/c are interpreted as being produced by a nucleon diffractive mechanism, whereas those events with $q_{\text{long}}{}^p > -2.0$ GeV/$c$ are considered pion diffractive. Following this division the various four-momentum transfer distributions were examined and found to be more or less peaked at small values, with sparsely populated tails. Cutoffs were made in the four-momentum transfers at points suggested by the data to delimit the tails; the data were reduced by less than 20% with these cuts. Subsequent analysis is confined to the regions listed in Table II. The cut sample is indicated by the hatched portion of the histograms in Fig. 2, nucleon and pion diffractive events by diagonal and cross hatching, respectively. The separation of the diffractive vertices in the cut sample is evidently unambiguous, there being no suggestion of a doubly diffractive contribution.[11] Moreover, the meson and nucleon distributions in Fig. 2 indicate that a double-peripheral approximation to the scattering amplitude might be appropriate.

Distributions in four-momentum transfers squared to the diffractive proton and pion are shown in Fig. 3, where the lines drawn through the data points represent slopes of 8 and 5 $(\text{GeV}/c)^{-2}$ for the proton and pion, respectively.

## DOUBLE-REGGE MODEL

The diagrams corresponding to the amplitudes used to parametrize the data in this experiment are shown in Fig. 4. The diffractive vertices are described by Pomeranchuk exchanges and characterized by exponential dependences on the four-momentum transfer squared at the vertices; the proton vertex is given by $e^{8t_{pp}}$, which is similar to elastic pion-nucleon scattering and the pion vertex has the form $e^{5t_{\pi\pi}}$. The nondiffractive vertices are approximated by pole terms; it is recognized that there is no unique low-energy form for the asymptotic Reggeized scattering amplitude and the adoption of the pole form with a constant residue for the vertex function is made on the basis of simplicity. Some authors prefer to represent the nondiffractive vertices by exponentials rather than poles[1,12]; either

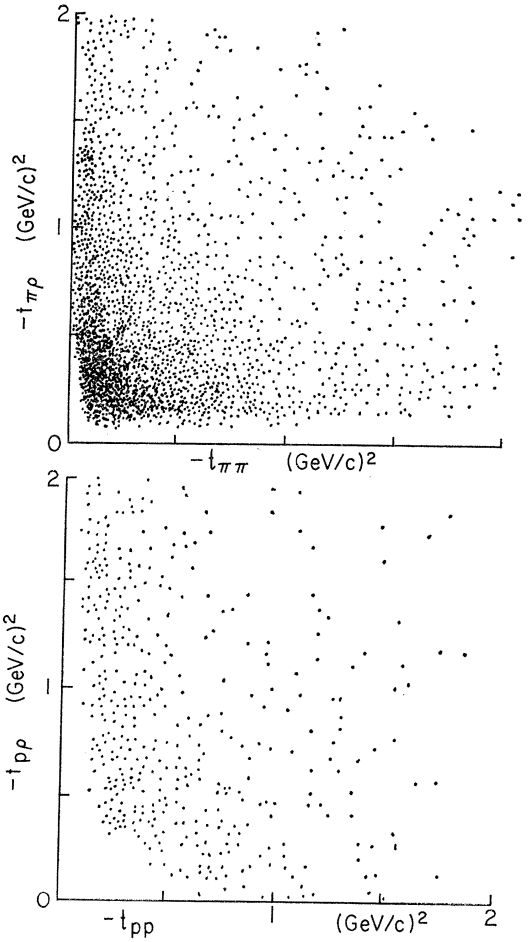


FIG. 5. (a) $-t_{\pi\rho}$ versus $-t_{\pi\pi}$ for the proton diffractive events. (b) $-t_{p\rho}$ versus $-t_{pp}$ for the pion diffractive events.

[11] For comments on double Pomeranchuk exchange and peripheralism in general see J. D. Jackson, rapporteur's report at the Lund Conference.

[12] J. W. Lamsa, J. A. Gaidos, R. B. Willmann, and C. R. Ezell, Phys. Rev. D 1, 3091 (1970).

form, when used in a double-Regge diagram, yields an essentially exponential dependence on the four-momentum transfer squared at the vertex. The pole form has one less input parameter and gives somewhat better description of the data. The residue is taken as a constant to be determined by normalization to the data. Modification of the nondiffractive vertices through the four-momentum dependence of spin factors has been ignored. The sum over the spin states for the proton diffractive amplitude yields smoothly varying functions over the regions studied, and does not alter the predictions of the pole form in any significant way. However, better agreement with the data was obtained by multiplying the residue by $t_{pp}$ in the case of nucleon exchange diagram b-IV of Fig. 4; possibly, this is a spin effect.

The Reggeized particle trajectory $\alpha_e(t)$ was taken as the linear form $\alpha_e(t)=J_e-m_e^2+\alpha_e'(0)t$, where $J_e$ and $m_e$ are the usual particle spin and mass. The slope $\alpha_e'(0)=1$ $(\mathrm{GeV}/c)^{-2}$ was applied for all trajectories. The Pomeranchuk trajectory was assumed to be given by $\alpha_{\mathrm{Pom}}=1.0$. Explicit dependence of the internal vertices on the Toller angle was ignored, the internal vertex coupling was taken as a constant.

The amplitude corresponding to the diagrams of Fig. 4 will be denoted by $A(a[b])$; the first letter in the parenthesis indicates the Reggeized particle exchanged and the bracketed letter $[b]$ refers to the diffractive particle to which the Pomeranchuk trajectory is coupled. With a similar notation for the normalization constants $N(a[b])$ for each diagram, the form adopted for the scattering amplitude illustrated by a-I of Fig. 4 is

$$A(\rho[p])=N(\rho[p])R_\rho(t_{\pi\pi})\times(s_{\pi\rho}/s_0)^{\alpha_\rho(t_{\pi\pi})}(s_{\pi p}/s_0)^{\alpha_{\mathrm{Pom}}}e^{8t_{pp}},$$

where $R_\rho(t_{\pi\pi})$ is the pole term

$$\{1-e^{i\pi\alpha_\rho(t_{\pi\pi})}\}/\{\Gamma(1+\alpha_\rho(t_{\pi\pi}))\sin[\pi\alpha_\rho(t_{\pi\pi})]\}$$

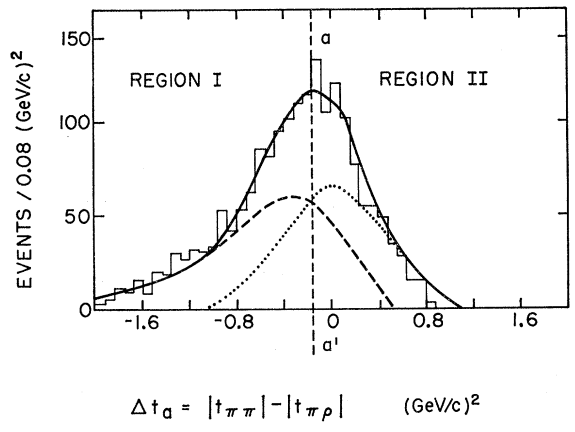


FIG. 6. Spectrum of $\Delta t_\alpha=|t_{\pi\pi}|-|t_{\pi\rho}|$; dashed curve is obtained from $A(\pi[p])$, the dotted curve from $A(\rho[p])$. Solid curve is the incoherent sum of the dashed and dotted curves.

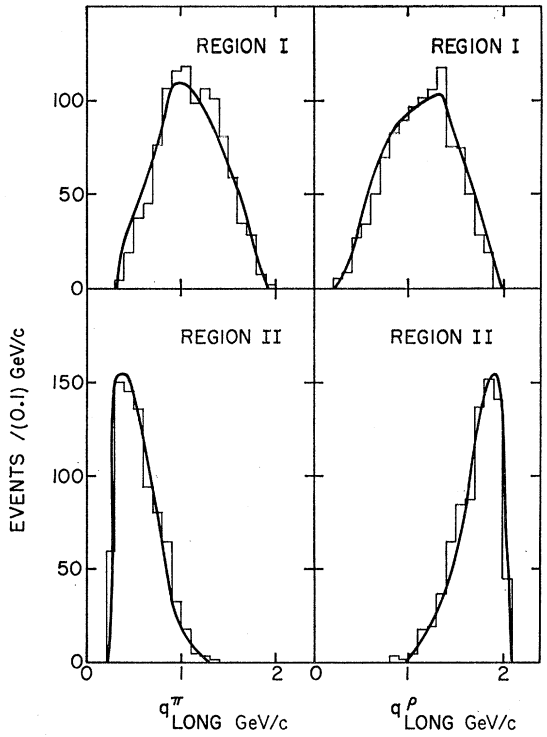


FIG. 7. Center-of-mass longitudinal momentum distributions of the pion and $\rho$ for regions I and II. Curves result from the double-Regge model.

and $s_0$ is the scaling energy, taken as 1.0 GeV$^2$ for all amplitudes. Specification of the four normalization constants $N(a[b])$ determines the contributions of the various amplitudes, with no adjustable parameters remaining.

All the diagram calculations in this paper were carried out by using the Monte Carlo phase-space program FOWL.[13] Many of the distributions presented are not independent, but are given to illustrate the over-all picture for this type of representation of the data and, perhaps, to find which variables are the most sensitive to small variations in assumptions.

## DIFFRACTIVE PROTON VERTEX

The necessity of including both diagrams of Fig. 4(a) to describe the scattering can be argued from the $-t_{\pi\rho}$ versus $-t_{\pi\pi}$ plot given in Fig. 5(a), where a strong clustering of events at simultaneously small values of the four-momentum transfers is clearly evident. Although each of the expressions corresponding to the diagrams of Fig. 4(a) gives a strong contribution when both four-momentum transfers are small, neither is applicable for the entire range under analysis. Since the only constraint applied to the values of $s_{\pi\rho}$, $s_{\pi p}$, or $s_{\rho p}$ in this analysis is $M(\pi^+p)>2.0$ GeV, the normalization of the diagrams is a nontrivial

[13] F. James, CERN Program Library (unpublished).

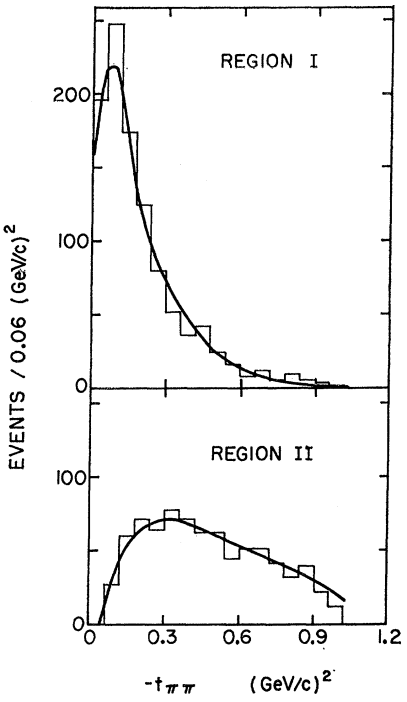


FIG. 8. Distributions in four-momentum transfer squared from the beam to the final pion. Curves are given by the double-Regge model.

problem because of the amount of overlap. Although both diagrams yield a substantial contribution in a common area of phase space, most of the regions are dominated by one only. For example, the Jackson angle of the pion in the $\pi$-$\rho$ center-of-mass system is peaked forward for the diagram a-I, whereas for a-II it is backward. An examination of the data reveals a nearly uniform distribution with some forward peaking, showing that both diagrams are required. Closely related to the Jackson angle is the difference $\Delta t_a = |t_{\pi\pi}| - |t_{\pi\rho}|$; the distribution of events in $\Delta t_a$ is given in Fig. 6. Contributions of diagrams a-I and a-II are shown by the dashed and the dotted curves, respectively, in Fig. 6; it is apparent that both contributions are needed to span the data. The solid curve in Fig. 6 is an incoherent sum of the dashed and dotted curves, which were approximately normalized to the tails of the data.[12]

Arguments derived from the concept of duality[14] between $s$- and $t$-channel scattering amplitudes imply that the data in the region where the diagrams both contribute strongly (see Fig. 6) can be described, on the average, equally well by either of the two graphs a-I or a-II. Furthermore, if the interference between the diagrams is included, the contributions have been improperly increased by double counting. We determine the normalization constants $N(\rho[p])$ and $N(\pi[p])$ and avoid double counting in the sense of duality by subdividing the data sample in the $\Delta t_a$ plot into disjoint phase spaces as indicated by the line $aa'$ drawn in Fig. 6. Events in region I are described by the diagram

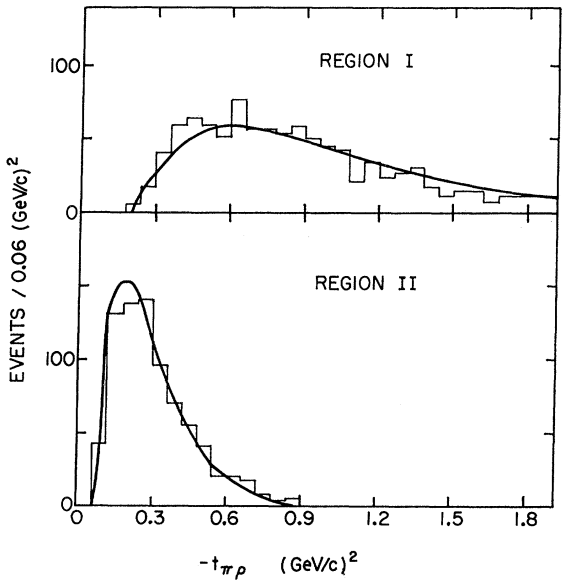


FIG. 9. Distributions in four-momentum transfer squared from the beam to the $\rho$. Curves result from the double-Regge model.

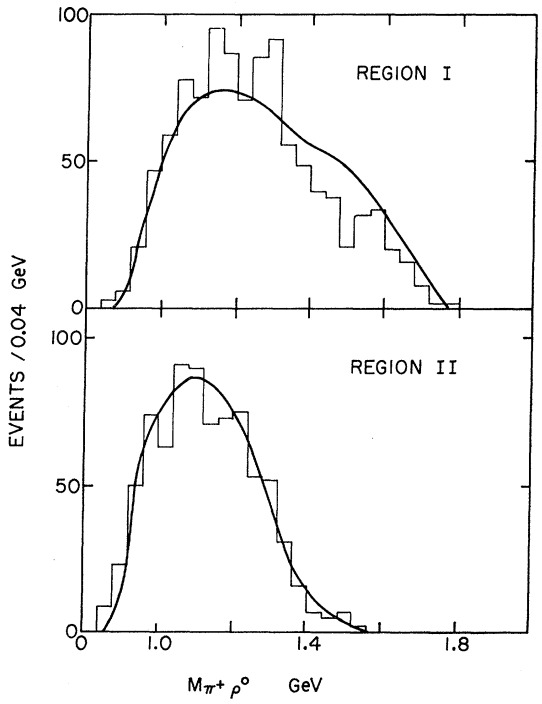


FIG. 10. Effective-mass distribution of the $\pi$-$\rho$ system with the curves from the double-Regge model.

[14] R. Dolen, D. Horn, and C. Schmid, Phys. Rev. 166, 1768 (1968); G. F. Chew and A. Pignotti, Phys. Rev. Letters 20, 1078 (1968).

a-I, whereas those in region II are described by a-II. Because both diagrams yield the same predictions for small $\Delta t_a$, the position of the line $aa'$ in the partition is not critical and was chosen at the point which roughly best separated the domains where a-I and a-II are dominant; this point is $\Delta t_a = -0.16$ GeV/$c^2$. The normalization constants are then readily determined by the number of events in the relevant region. In this experiment, with $aa'$ as drawn, region I contains 1036 events, region II 792 events.

## RESULTS

The center-of-mass longitudinal momentum distribution of the pion and $\rho$ meson are shown separately for the two regions in Fig. 7; the solid curves are the prediction of the amplitudes $A(\rho[p])$ and $A(\pi[p])$ for regions I and II, respectively, normalized to the number of events in each region. It is observed that the single-particle distributions are described quite well by the model.

Four-momentum transfers squared to the pion, $t_{\pi\pi}$, and to the $\rho$ meson, $t_{\pi\rho}$, are given in Figs. 8 and 9. The $\rho$-$\pi$ mass spectrum is shown in Fig. 10; the model provides a good description of the low-mass peaking, with perhaps a suggestion that there is some direct resonance production in region I. The two diagrams overlap almost entirely over the $\pi$-$\rho$ mass spectrum; consequently, amplitudes which yield a poor representation in other variables can give an adequate descrip-

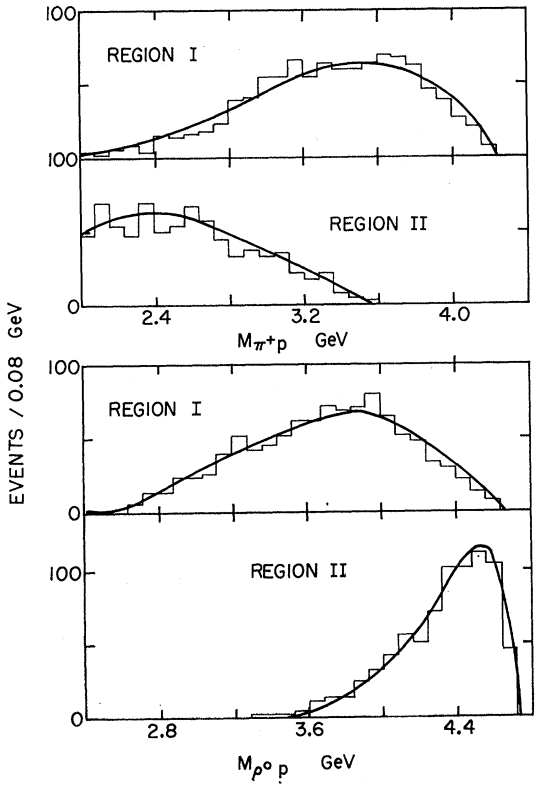


FIG. 11. Effective-mass distributions of the pion-proton and the $\rho$-meson–proton systems with curves from the double-Regge model.

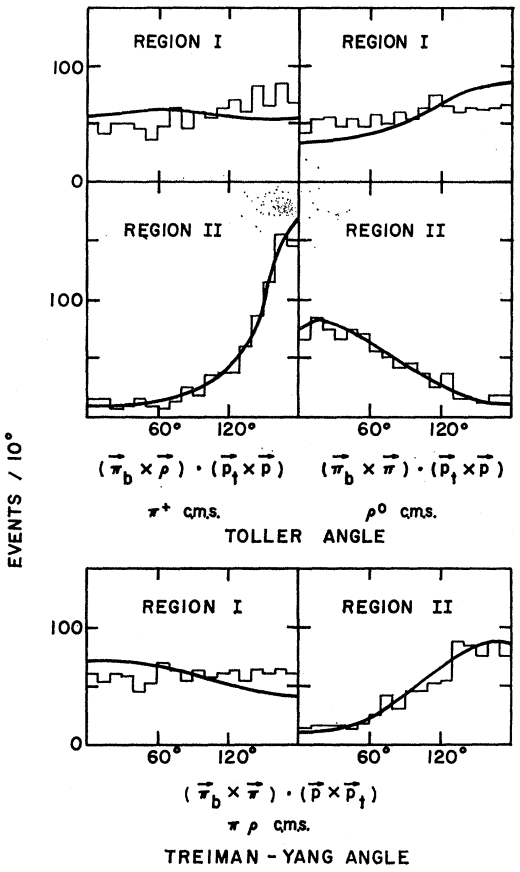


FIG. 12. Distributions of the Toller angle and the Treiman-Yang angle. Curves result from the double-Regge model.

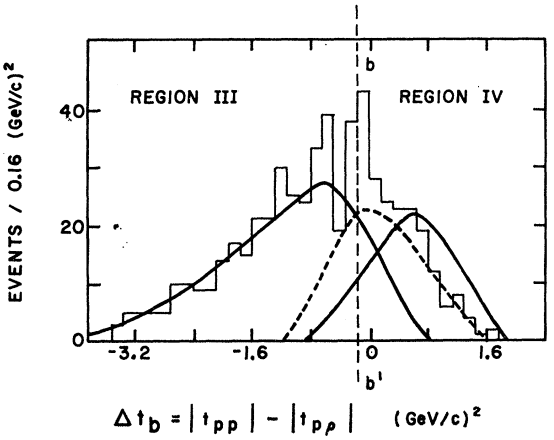


FIG. 13. Spectrum of $\Delta t_b = |t_{pp}| - |t_{p\rho}|$; solid curves are obtained from $A(\rho[\pi])$ and $A(p[\pi])$ for regions III and IV, respectively, the dashed curve from $A(p[\pi])$.

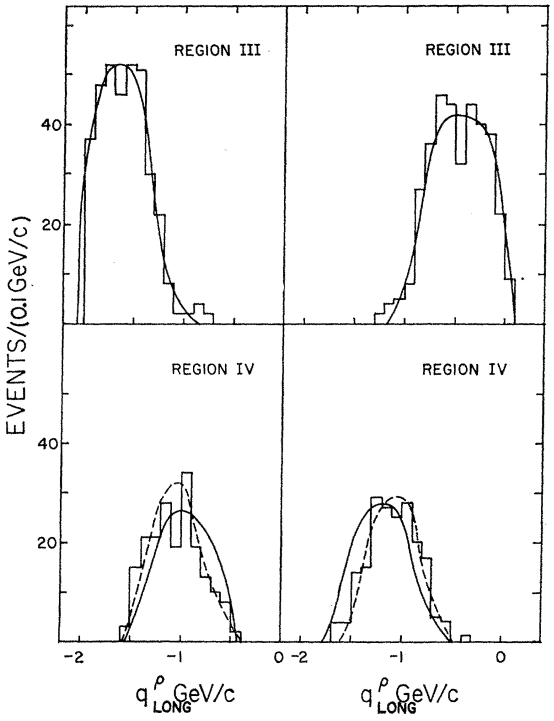


FIG. 14. Center-of-mass longitudinal momentum distributions for regions III and IV. Curves are given by the double-Regge model.

tion of the $\pi$-$\rho$ mass distribution by some compensation. The leading edges of the histograms in Fig. 10 consist primarily of those events in the strong cluster region of Fig. 5, and are in good agreement with the shapes given by the model.

Distributions and comparisons of the pion-nucleon and the $\rho$-meson–nucleon masses are displayed in Fig. 11, where the agreement with predictions is seen to be very good. In Fig. 12 the distributions of the Toller angles in the pion center of mass and in the $\rho$-meson center of mass are shown along with the Treiman-Yang angle in the $\pi$-$\rho$ system. The model reproduces the data well; in particular, the skewed Treiman-Yang spectrum in region II is correctly described.

The amplitudes derived by Berger[15] for diagrams a-I and a-II were also calculated and compared with the simple pole model. The predictions of the Berger model are not significantly different from those of the simple pole approximation within the ranges of the variables studied here.

## PION DIFFRACTIVE VERTEX

A scatter plot of $-t_{pp}$ versus $-t_{p\rho}$ shown in Fig. 4(b) also exhibits a clustering at small values, although not as markedly as in the previous case of proton diffraction [Fig. 4(a)]. The distribution in $\Delta t_b = |t_{pp}| - |t_{p\rho}|$ is presented in Fig. 13, where a peaking at low $\Delta t_b$ values is apparent. The solid curves in Fig. 13 represent calculations of $A(\rho[\pi])$ and $A(p[\pi])$ corresponding to diagrams b-III and b-IV of Fig. 4. The dashed curve is obtained by introducing a $t_{p\rho}$ factor into the residue of $A(p[\pi])$, i.e., $A(p[\pi]) \rightarrow t_{p\rho}A(p[\pi])$, which amplitude will be denoted by $\bar{A}(p[\pi])$. There is some precedent in Regge-pole theory for introducing *ad hoc* $t$ factors in residues and it is evident in Fig. 13 that $\bar{A}(p[\pi])$ better describes the data in region IV. An examination of Fig. 13 makes clear the necessity of

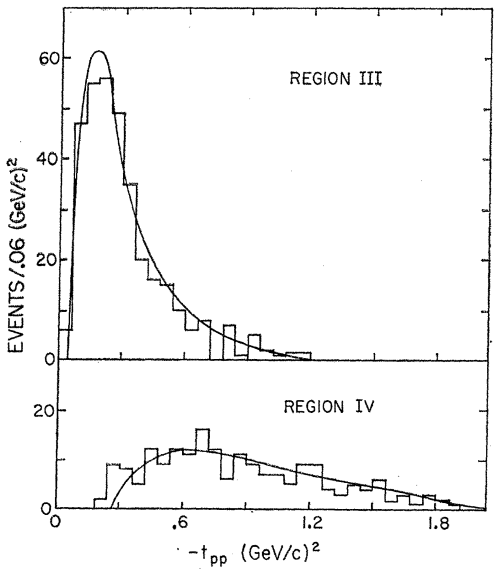


FIG. 15. Distributions of four-momentum transfer squared from the target proton to the final proton. Curves are from the double-Regge model.

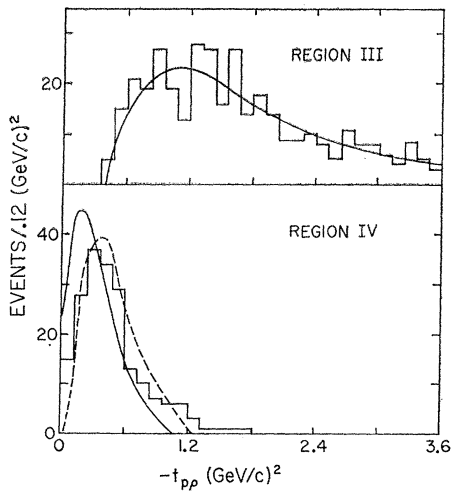


FIG. 16. Distributions of four-momentum transfer squared from the target proton to the $\rho$ meson. Curves are from the double-Regge model.

[15] E. L. Berger, Phys. Rev. 166, 1525 (1968).

including both diagrams b-III and b-IV of Fig. 14. The data is again subdivided by the line $bb'$ at $\Delta t_b = -0.16$ GeV/$c^2$ into two regions, III and IV; region III contains 357 events, region IV 193 events.

Center-of-mass longitudinal momentum distributions of the $\rho$ meson and proton are shown in Fig. 14, where the solid curves are obtained from $A(\rho[\pi])$ and $A(p[\pi])$ for regions III and IV and normalized to the number of events in their respective regions. $\bar{A}(p[\pi])$ is represented by the dashed line, and offers a better approximation to the behavior of the data in region IV.

Four-momentum transfers squared $-t_{pp}$ and $-t_{p\rho}$ are given in Figs. 15 and 16. The dashed curve in region IV of Fig. 16 is the prediction of the modified amplitude $\bar{A}(p[\pi])$.

Mass distributions are given in Fig. 17 with model predictions of $A(\rho[\pi])$ and $A(p[\pi])$ shown by the solid curves. The dashed line representing $\bar{A}(p[\pi])$ is drawn only if the results of $A(p[\pi])$ and $\bar{A}(p[\pi])$ are significantly different. The agreement is generally good, with a sharp rise in region IV of the $M(p\rho)$ spectrum at least partly due to a 10% contribution of a $\Delta^{++}$ state formed between the positive pion in the $\rho$ and the final proton. Angular distributions are given in Fig. 18, where again the data are well described by the model.

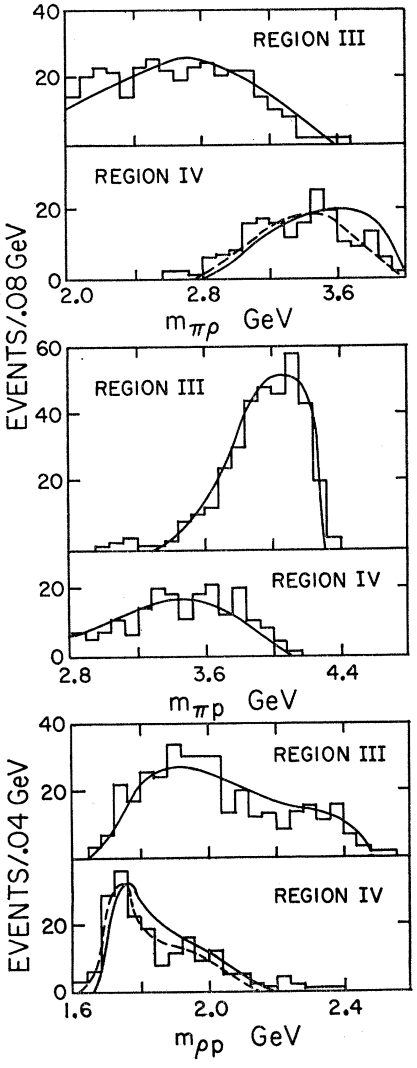


FIG. 17. Effective-mass distributions of the $\pi$-$\rho$, $\pi$-$p$, and $\rho$-$p$ systems. Curves are from the double-Regge model.

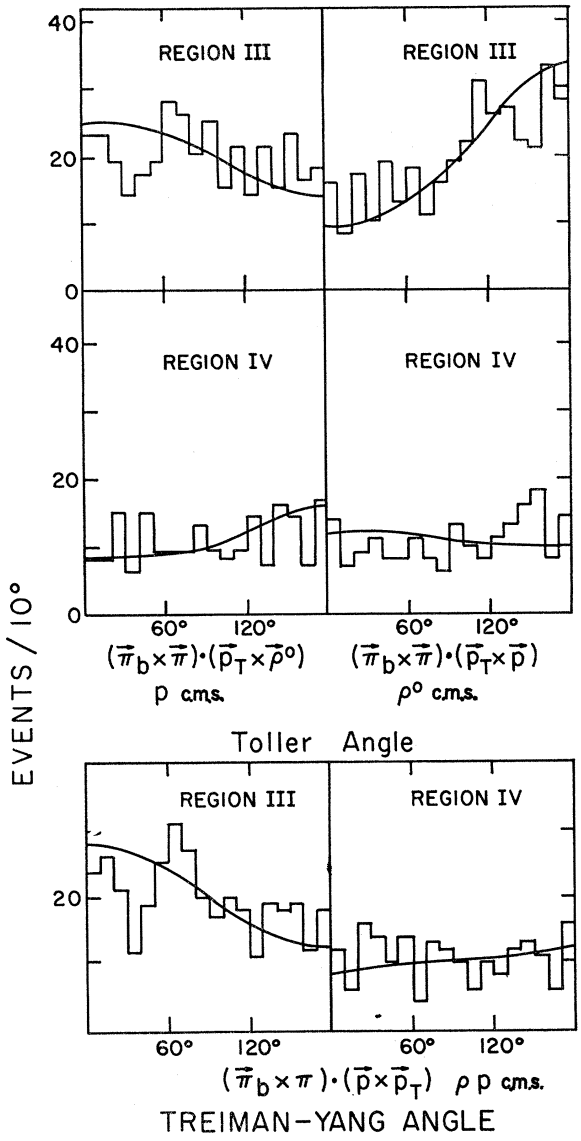


FIG. 18. Distributions of the Toller angle and the Trieman-Yang angle. Curves result from the double-Reggemodel.

## SUMMARY

The reaction $\pi\pi^+ p \to \pi^+ \rho^0 p$ at 13.1 GeV/$c$ for $m_{\pi^+ p} > 2$ GeV can be described in terms of diffractive scattering off the target proton (~80% of the events) or off the

incident pion ($\sim 20\%$ of the events). With modest restrictions of the four-momentum transfer ranges, the data are well described by a double-Regge approximation where the nondiffractive vertices are represented by a constant residue and a pole. Phase space is separated into two regions, each of which is assumed to be dominated by one exchange diagram; thus the model can be applied without high-mass restrictions, and double counting in the sense of duality is avoided. Since each region was independently well described by the model, the data for each distribution can be summed over the two regions spanned and can maintain the quality of the description if the diagrams are added incoherently.[10]

The low-mass enhancement in the $A$ region is effectively reproduced by the amplitudes in the $t$ channel corresponding to diagrams a-I and a-II as suggested by semilocal duality.

PHYSICAL REVIEW D VOLUME 2, NUMBER 7 1 OCTOBER 1970

# A Study of the $K\pi\pi$ System in $K^-p \to K^-\pi^+\pi^-p$ at 12.6 GeV/$c$*

T. LUDLAM, J. SANDWEISS, AND A. J. SLAUGHTER
*Yale University, New Haven, Connecticut 06520*

(Received 15 June 1970)

The $K\pi\pi$ spectrum in the reaction $K^-p \to K^-\pi^+\pi^-p$ at 12.6 GeV/$c$ is analyzed, taking as a starting point the observation that the transverse momentum distributions are uniform throughout this spectrum and are restricted to small values. This behavior results in a threshold enhancement in the $K\pi\pi$ spectrum corresponding to every $K\pi$ mass value. With the exception of the $Q$ peak, and perhaps the $L$ meson, the $K\pi\pi$ mass spectrum can be regarded as a continuous sequence of such enhancements, which follow from phase-space distributions in the longitudinal momenta. A double-Regge-pole-exchange model for the $Q$ gives qualitative agreement with the data, but only if at least two exchange amplitudes are included; it does not give a correct description of the detailed correlations between the longitudinal and transverse momenta. A more successful description is given by a very simple resonance model. The similarities between the predictions of these two models—which are related by the concept of duality—are discussed in terms of the kinematic restrictions imposed by the condition of small transverse momenta.

## I. INTRODUCTION: SOME CHARACTERISTIC FEATURES

RECENTLY, experimenters with high-energy bubble-chamber data have devoted considerable attention to threshold boson enhancements in reactions like

$$M+T \to (M\pi\pi)+T, \tag{1}$$

where $M$ represents an incident meson and $T$ a nucleon target. The threshold enhancements in the $M\pi\pi$ system result, presumably, from diffraction dissociation of the incident beam particle, and are seen only when two of the outgoing mesons combine to form a resonant state. For incident $\pi$ mesons, the observed enhancements are $A_1$ ($\rho\pi$) and $A_3$ ($f\pi$), and for incident kaons one observes the $Q$ ($K^*(890)\pi$; $K\rho$) and $L$ ($K^*(1420)\pi$). In the cases of the $Q$ and $A_1$, very detailed analyses of the experimental data have been performed—with considerable success—from each of two apparently divergent points of view: (i) assuming a double-peripheral $t$-channel exchange amplitude (Deck effect), and (ii) assuming the observed enhancements to consist primarily of peripherally produced resonant states of definite spin and parity.[1] The principle of duality, as demonstrated in the case of two-body final states by Dolen, Horn, and Schmid,[2] is usually invoked to reconcile the apparent equivalence of these two approaches in understanding the experimentally observed phenomena.

In this paper we examine the behavior of the $K\pi\pi$ system in the reaction

$$K^-p \to K^-\pi^+\pi^-p \tag{2}$$

for an incident kaon momentum of 12.6 GeV/c. The data to be discussed are from an investigation of 1291 examples of reaction (2) in an exposure of the BNL 80-in. bubble chamber to a beam of 12.6-GeV/$c$ rf-separated $K^-$ mesons. The $K^-\pi^+$ and $K\pi\pi$ mass spectra for this reaction are shown in Fig. 1. In Fig. 1(a), the $K^*(890)$ peak is seen to dominate the reaction. A small $K^*(1420)$ peak is also present. The $K\pi\pi$ spectrum has as its most obvious feature the $Q$ peak, which re-

* This work [Yale Report No. 2726-580 (unpublished)] is supported by the U. S. Atomic Energy Commission under Contract No. AT(30-1)2726. The authors hold guest appointments at Brookhaven National Laboratory, Upton, New York.

[1] A recent review of the analysis of the $Q$ and $A_1$ peaks, with extensive references, is given by M. Derrick, in *Proceedings of the Boulder Conference on High-Energy Physics*, edited by K. T. Mahanthappa, W. D. Walker, and W. E. Brittin (Colorado A.U.P., Boulder, 1970), p. 291. Some controversy exists as to whether the $L$ meson is entirely the result of threshold production of $K^*(1420)+\pi$. See the review by C. Y. Chien, in Johns Hopkins University Report No. JHU-7010, 1970 (unpublished).

[2] R. Dolen, C. Horn, and D. Schmid, Phys. Rev. **166**, 1768 (1968); G. Chew and A. Pignotti, Phys. Rev. Letters **20**, 1078 (1968).